

NUMERICAL SIMULATION OF MICROSTRUCTURE EVOLUTION OF BINARY ALLOYS DURING THE SOLIDIFICATION PROCESS

Ever Grisol de Melo

Alexandre Furtado Ferreira

Universidade Federal Fluminense, Volta Redonda / RJ
 ever_egm@hotmail.com , furtado@metal.eeimvr.uff.br

Abstract. *The understanding solidification process of metals and alloys is very important because the microstructures control the segregation and consequently determine the properties of the materials. The microstructures arise during the solidification process of alloys in the super-cooling domain, while solutes are rejected from solid to the liquid.*

In this present paper we applied the phase-field model based on the Finite-Difference Method, for study the effects in change of carbon concentration on the microstructure shapes. The influence of different super cooling levels on the microstructure shapes are studied too. The profiles of carbon concentration are calculated by phase-field model for both the solid and liquid phase. The results show good agreement with those found in literature on the solidification.

Keywords: *Dendrite; Modeling; phase-field mode*

1. INTRODUCTION

The solidification is one of the most important specialty metals and its industrial study is a powerful tool, since it provides the shortest distance from raw material to end product. The understanding the solidification process of metals and alloys is essential to determine properties of materials, because microstructures evolution control the segregation process. The dendritic microstructures arise during the solidification of alloys, while solutes are rejected from solid to the liquid phase in super-cooling domain.

This compression process is essential because the nucleation and dendritic growth influence on the properties of the final product.

The nucleus was previously added to the system, which may be stable under the conditions of the system super-cooling (ΔT) and solute concentration.

In method, thickness of the interface is important as a parameter ϵ_0 correlates with the actual thickness of the interface. This parameter was calculated simultaneously to get closer to reality, with λ and W .

In this paper, all equations were solved numerically using the finite difference method with an explicit scheme. In this present work, we study the effects for different levels of super-cooling and carbon concentrations on the morphology of the microstructure through a single seed previously added to the liquid region. The model reproduces the general behavior found in the literature on solidification.

2. PHASE-FIELD MODELING FOR ALLOYS FE-C

The solution of energy, concentration and phase-field equations is done by the phase-field model. Phase-field modeling assumes the growth of seeds in the liquid phase with three regions: the solid nucleus, the liquid phase and the solid/liquid interface.

The state of the entire domain is represented by the distribution of a single variable known as the order parameter, ϕ , or phase-field variable. The solid material is represented by $\phi = 1$ while, in the liquid region, $\phi = 0$. The region in which ϕ changes from 1 to 0 is defined as the solid/liquid interface. The time evolution equation of the phase-field ϕ is described by :

$$\frac{\partial \phi}{\partial t} = M \left(\begin{array}{l} \epsilon(\theta)^2 \nabla^2 \theta + \frac{\delta}{\delta y} \left(\epsilon(\theta) \cdot \epsilon'(\theta) \frac{\delta \phi}{\delta x} \right) - \frac{\delta}{\delta x} \left(\epsilon(\theta) \cdot \epsilon'(\theta) \frac{\delta \phi}{\delta y} \right) - W g'(\phi) \\ - h'(\phi) \frac{RT}{Vm} \ln \left[\frac{(1-c_s^e)(1-cl)}{(1-c_l^e)(1-cs)} \right] \end{array} \right) \quad (1)$$

where M is defined as the solid/liquid interface mobility, the angle θ is given by the orientation of a vector perpendicular to the solid/liquid interface, e.g., $\nabla \phi$. ΔH is the latent heat and T_m the melting temperature. The function $g'(\phi)$ that multiplies w determines the distribution of the excess free-energy at the interface. $h'(\phi)$ is a function that satisfies the condition $h'(0) = h'(1) = 0$.

Grisol Melo E. , Ferreira A.F.

Numerical simulation of micro structure evolution of binary alloys during the solidification process

$$h(\phi) = \phi^3(6\phi^2 - 15\phi + 10) \quad (2)$$

$$g(\phi) = \phi^2(1 - \phi^2) \quad (3)$$

Equations (2) and (3) are widely used in combination with the Phase-field Method. Note that the term $Wg'(\phi) - h'(\phi) \frac{RT}{V_m} \ln \left[\frac{(1-c_s^e)(1-cl)}{(1-c_l^e)(1-cs)} \right]$

is $\phi = 0$, in which case only liquid is present and when $\phi = 1$, only solid is present. As expected, this term is different from zero only in the presence of both the solid and liquid phases.

In the calculations of the equation metal alloy phase change according to the angle θ , taking into account the interface as its instability and the anisotropy of the solidified alloy. For this the value of the parameter $\varepsilon(\theta)$ is a function of the angle of advance of dendrite orientation relative to axis \mathbf{x} by the equation:

$$\theta = \text{artg} \left(\frac{\theta_y}{\theta_x} \right) \quad (4)$$

Resulting in parameter $\varepsilon(\theta)$:

$$\varepsilon(\theta) = \varepsilon(1 + \delta_\varepsilon \cos j(\theta - \theta_0)) \quad (5)$$

$$\sigma = \frac{\varepsilon \sqrt{W}}{3\sqrt{2}} \quad (6)$$

$$2\lambda = 2.2\sqrt{2} \frac{\varepsilon}{\sqrt{W}} \quad (7)$$

δ_M is the anisotropy constant, \mathbf{j} controls the number of preferential directions of the material's anisotropy, as 0 for the isotropic cases as 4 for anisotropy of 4 directions. The constant θ_0 is the interface orientation with respect to the maximum anisotropy, while ε and w are parameters associated with the interfacial energy (σ) and interface thickness (λ), as proposed by Boettinger.

The mobility parameter of the interface is represented by M according to Ode et al. Are calculated simultaneously:

$$\frac{1}{M} = \sigma \varepsilon^2 \left\{ \frac{\beta RT(1-K_e)}{V_m \cdot m_e} + \frac{\varepsilon \zeta(C_s, C_l)}{D \sqrt{2W}} \right\} \quad (8)$$

The term β is the relative interfacial kinetic coefficient μ_k , R is the gas constant, T temperature, V_m is the molar volume, m_e is the slope of the liquidus in the phase diagram and the diffusivity D of the interface. Since interface for energy and kinetic coefficient will depend on the preferred direction of growth anisotropy is one of the parameters for the morphology of the interface. The term $\zeta(C_s, C_l)$ represents the concentration ratio by the equation:

$$\zeta(C_s, C_l) = \frac{RT(C_s^e, C_l^e)}{V_m \cdot m_e} \times \int_0^1 \frac{h(\phi)(1-h(\phi))}{((1-h(\phi))C_l^e(1-C_l^e) + h(\phi)C_s^e(1-C_s^e)) \cdot \phi(1-\phi)} \cdot d\phi \quad (9)$$

The term C_s^e is concentration of the solid in equilibrium and C_l^e is concentration of the liquid in equilibrium.

The dendritic growth is by a term that represents the disruption of the solidification interface. The values of this term will be through a random generator, as Warren and Boettinger and study by Furtado.

$$\text{Noise} = 16 a r \phi^2(1 - \phi)^2 \quad (10)$$

a is the factor of the amplitude of the noise, r is generate the random number. Note that it is only the noise generated at the interface region because when the values of ϕ is 0 or 1, the term is zero.

For the equation of concentration, we will take into account the initial concentration of the alloy as a function of $C = C_0 K_e$, to C_0 the initial concentration and the distribution coefficient K_e of the alloy. Immediately concentration equation is as follows:

$$\frac{\partial c}{\partial t} = \nabla \left[D(\phi) \left[(1 - h(\phi)) c_l (1 - c_l) + h(\phi) c_s (1 - c_s) \right] \nabla \ln \left(\frac{c_l}{c_s} \right) \right] \quad (11)$$

To calculate the concentrations of the liquid and solid at the moment equilibrium equations is adopted:

$$C_l^{eq} = \frac{T_m - T}{M_e} \quad (12)$$

$$C_s^{eq} = (T_m - T) \frac{K_e}{M_e} \quad (13)$$

3. RESULTS AND DISCUSSION

“Table 1” presents the physical properties of the binary alloy (Fe-C) used in the computations that follow. The parameters used in the phase-field model obtained of physical properties of the material were derived from Equation (6) to (9). “Table 2” presents these parameters.

The boundary condition adopted for the phase-field model (ϕ) in this work is a zero-flux condition.

Table 1. Physical properties of Fe-C alloys.

Properties	C	Fe
Initial concentration [%mol]	6.48×10^{-3}	
Partition coefficient, K_e	0.204	
Slope of liquidus line, M_e [$K \text{ mol}^{-1}$]	1836	
Diffusivity in solid region, D_s [$\text{m}^2 \text{ s}^{-1}$]	6×10^{-9}	
Diffusivity in liquid region, D_l [$\text{m}^2 \text{ s}^{-1}$]	2×10^{-8}	
Molar volume, V_m [$\text{m}^3 \text{ mol}^{-1}$]		7.7×10^{-6}
Melting temperature, T_m [K]		1810
Interface energy, σ [J m^2]		0.204

Table 2. Computational parameters.

Anisotropy, $\delta\varepsilon$	0.03
Interface thickness, ε_0 [J m^{-1}] ^{1/2}	1.055×10^{-3}
Surface tension, W [J m^{-3}]	673.2×10^3
Interface mobility, M [$\text{m}^3 \text{ s}^{-1}$]	1.551×10^{-6}
Time-steps length, Δt [s]	3.1×10^{-6}
Grid spacing, $\Delta x = \Delta y$ [m]	0.5×10^{-6}
Noise amplitude, a	0.02

To calculate the governing equations, there are seven unknown values. The three of them are phase-field parameter. Both of \mathbf{W} and $\boldsymbol{\varepsilon}$ are determined by solving the eqs. (6,7) and (8) simultaneously. Since the phase-field mobility is a function of temperature, it should be calculated with the temperature during the computation. The value of carbon concentration in liquid c_l and solid c_s are also required. They are determined from eq. (12,13) depending on the ϕ and \mathbf{c} at each point and at every time step. The governing equations, eqs. (1) and (11), are numerically solved using a finite difference scheme. In the calculations the system temperature is uniform and continuously decreased with a constant cooling rate from the initial temperature (T_0), which is slightly lower than the liquidus temperature of the Fe-C alloy.

We analyze the dendrite growth in tow-dimensional system. The dendrite shapes of Fe- 5.87×10^{-3} mol% C and Fe- 6.87×10^{-3} mol% C binary alloys at 1800 K are shown in “Fig. 1”. The concentration field, during dendritic growth is shown in “Fig.1”. In the figure, the gray scale represents solute concentration, while the white represents the concentration of the segregated carbon from solid to liquid region. The carbon concentration in solid is much less than that of carbon in liquid. The secondary arms develop well and spacing increases with a little additional carbon (Figure 1a and b), because of carbon enrichment at the interface and reduction of interface stability. With increase in carbon concentration, the Fe-C dendrite becomes narrower.

Grisol Melo E. , Ferreira A.F.

Numerical simulation of micro structure evolution of binary alloys during the solidification process

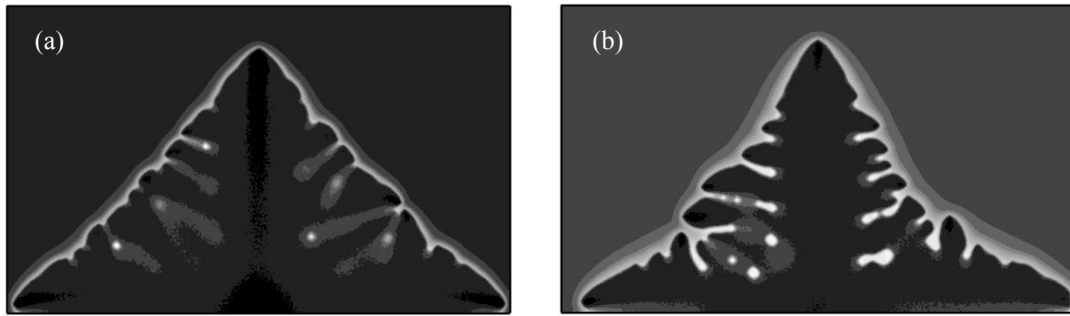


Figure 1. Calculated concentration profiles in solid and liquid region during solidification of Fe-C alloy ($T_0 = 1800$ K) and Initial concentration of (a) 5.87×10^{-3} mole fraction and (b) 6.87×10^{-3} mole fraction.

“Figure 2” shows the concentration profiles across vertical symmetry axis obtained from the phase-field simulation, “fig. 1”. Note that concentration profiles are not fully horizontal, thus showing evidence of microsegregation. Also, it can be seen how the concentration profile from the phase-field simulation varies within the interfacial region, in each curve, there is a sharp increase in concentration in the interface region. This occurs due to the increase of the carbon concentration from 5.86×10^{-3} to 6.86×10^{-3} . At each curve, the concentration profiles in the solid region follows $C_s = K_e \cdot C_L$ law in the phase field formulation, while decays exponentially toward initial concentration in liquid region ahead of the solid/liquid interface. The thickness of the diffusion boundary layer in the liquid region becomes smaller with lower carbon concentration because of the higher interface velocity. As the carbon concentration decreases, the ratio of the solid concentration to the liquid concentration at the interface increases, i.e. solute trapping effect becomes more pronounced.

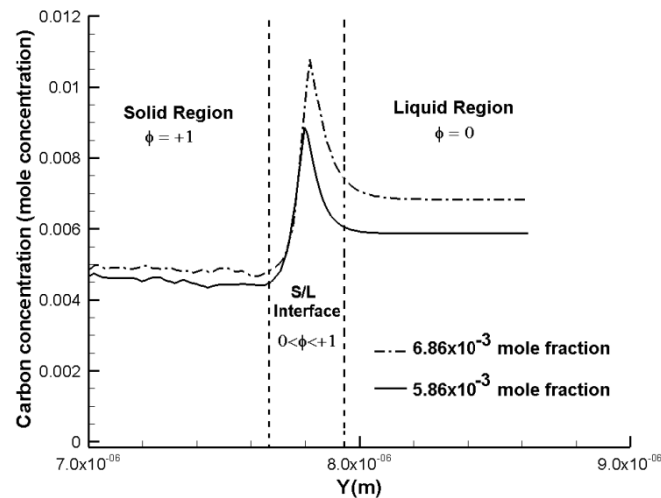


Figure 2. Carbon concentrations by region: solid ($\phi = +1$), liquid ($\phi = 0$), and interface ($0 < \phi < +1$).

“Figure 3” shows the morphology of dendrites which are calculated at the concentration of 6.87×10^{-3} mole fraction for different initial temperatures 1798 K and 1802 K. This figure shows similar microstructural features which can be found in “Fig. 1”. The increase in temperature at a fixed carbon concentration results in a similar effect on the dendritic structure as being decreased in composition of alloy. “Figure 3 (a) and 3 (b)” are similar to “Figs. 1(a) and 1(b)” respectively. The dendrites are calculated by phase field model, where a constant temperature gradient is imposed in an undercooled melts system. The simulation of the dendritic evolution is achieved by disregarding the energy equation and instead imposing the following linear temperature profile:

$$T(t) = T_0 - \dot{T} \quad (14)$$

The constant value of cooling rate \dot{T} was adopted as 83.33 K/s from the experimental data.

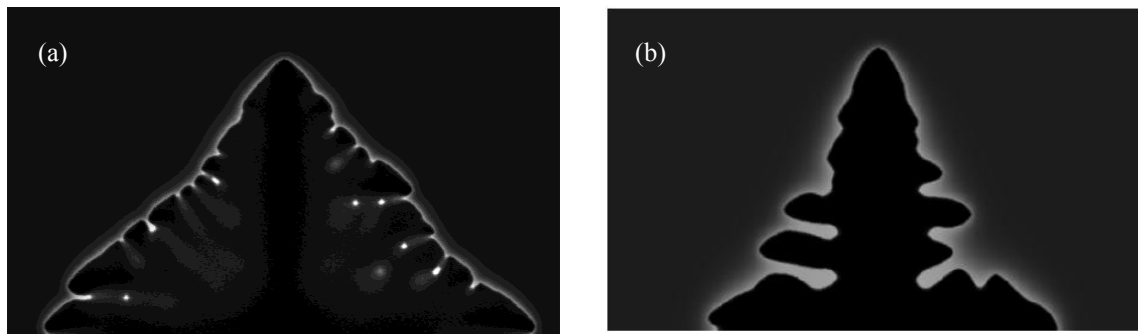


Figure 3. Calculated dendritic shapes during isothermal solidification of Fe-C alloy with fixed composition of 6.87×10^{-3} mole fraction and initial temperature of (a) 1798 K and (b) 1802 K.

4. CONCLUSIONS

The phase-field model for binary alloys is applied to the numerical prediction of the dendrite growth in Fe-C. The results seem to be quite reasonable and show the wide potentiality of phase field model to the simulations of the dendrite growth in the undercooled systems. Two-dimensional simulations produced dendrites, which are similar to the ones found in experiments reported in the literature, complete with primary and secondary arms. With increase in carbon concentration, the Fe-C dendrite becomes narrower. The increase in temperature at a fixed composition results in a similar effect on the dendrite geometry.

5. ACKNOWLEDGEMENTS

The authors would like to thanks FAPERJ/APQ1 (No. E-26/111.930/2012) by financially supported.

6. REFERENCES

- Boettinger, W.J., Wheeler A.A. and McFadden G.B., 1992. "Phase-Field model for isothermal phase transitions in binary alloys", *Physical Review A*, vol. 45, p 7424-7439.
- Ferreira, A.F. and Ferreira, L.O., 2009. "Microsegregation in Fe-C-P Ternary Alloys Using a Phase-Field Model", *Journal of the Brazilian Society of Mechanical Sciences and Engineering*. Vol. XXI, p. 173-180.
- Ferreira, A.F., Silva A.J. and Castro J.A., 2006. "Simulation of the solidification of pure nickel via the phase-field method", *Materials Research*. Vol.9, n° 4, p. 349-356.
- Garcia A., 2007. "Solidificação: Fundamentos e Aplicações (Solidification: Fundamentals and Applications)", *Ed. Unicamp*. Campinas, Brazil.
- Kim S.G., Kim W.T., Lee J.S. and Ode M., Suzuki T., 1999. "Numerical Simulation of Isothermal Dendritic Growth Phase-field Model", *ISIJ International*, Vol.39, p. 335.
- Kobayashi, R., 1993. "Modeling and numerical simulations of dendritic crystal growth", *Physical D*. Vol. 63, p. 410-423.
- Lee J.S. and Suzuki T., 1999. "Numerical simulation of isothermal dendritic growth by phase-field model", *ISIJ International*. Vol. 39, p. 246-252.
- Ode M., Kim S.G., Kim W.T. and Suzuki, T., 2001. "Numerical Prediction of the Secondary Dendrite Arm Spacing Using a Phase-field Model", *ISIJ International*. Vol. 41, n° 4, p. 345-349.
- Ode M., Lee J.S., Kim S.G., Kim W.T. and Suzuki T., 2000. "Phase-field Model for Solidification of Ternary Alloys", *ISIJ International*. Vol. 40, n° 9, p. 870-876.
- Ode M., Lee J.S., Suzuki T., Kim S.G. and Kim W.T., 2000. "Investigation of the Mechanism of Alloy Dendrite Deflection due to Flowing Melt by Phase-Field Simulation", *ISIJ International*, vol. 40, n° 9, p 870.
- Salvino, I.M., Ferreira L.O. and Ferreira A.F., 2012. "Simulation of Microsegregation in Multicomponent Alloys During Solidification", *Steel Research International*. Vol. 83, p. 723-732.

7. RESPONSIBILITY NOTICE

The authors are the only responsible for the printed material included in this paper.